OG 4.1.20

Silicon Matrix Detector for ATIC

J.H. Adams, Jr.[1], J. Ampe[1], G. Bashindzhagyan[2], O. Ganel[3], R. Kroeger[1], E. Kuznetsov[2], M. Panasyuk[2], G. Samsonov[2], E.S. Seo[3], A. Voronin[2], D. Wagner[1], J.Z. Wang[3], and V. Zatsepin[2] for the ATIC Collaboration

[1] *Naval Research Laboratory, Washington, DC 20375, USA*

[2] *Skobeltsyn Institute, Moscow State Univ., Moscow 119899, Russia*

[3] *Univ. of Maryland, College Park, MD 20742, USA*

Abstract

We report on the first large-area silicon matrix developed for cosmic ray research. The ATIC silicon matrix is 1 square meter array of silicon detectors that detects all cosmic rays within the entrance aperture of ATIC and separates the individual elements from H to Fe. It consists of 4480 separate detector pads that are separately read out using a custom VLSI chip and digitized to 12-bit precision.

1 Introduction:

The silicon matrix is designed to provide individual charge resolution from H to Fe for the Advanced Thin Ionization Calorimeter (ATIC) experiment (Guzik et al., 1999). It must detect all incident particles within the ATIC aperture, including those incident at zenith angles up to 57°. To separate the lightest elements, care must be taken about the additional signal due to radiation scattered back from the calorimeter. For this reason the matrix must be a mosaic of small detector pads so that the pad containing the signal from the incident particle is likely to have little or no additional signal. Simulations of ATIC have shown that for detector pads as small as 3 cm^2, the fraction of misidentified protons is less than 2% in the energy range 10 GeV to 100 TeV due to backscatter (Seo et al., 1996 and Ganel et al. 1999).

2 Matrix Design:

The matrix consists of four planes of detectors. The active detector areas in these planes are partially overlapped to completely cover the aperture. The matrix is built from four-pad silicon detectors mounted on daughter boards with 28 daughter boards mounted on a motherboard. The motherboards are multi-layer circuit boards 109 cm long and 6.634 cm wide (Universal Circuits, 1999) that also carry the front-end electronics for the detectors. Detector ladders consist of two motherboards with one inverted over the other and offset so the active detector areas partially overlap. The matrix has two panels of ladders with 10 ladders on each. These panels face each other with the ladders mounted offset so that the active areas of the ladders partially overlap. The active area of the matrix is 99.2 cm by 111.2 cm.

2.1 Silicon Detectors: The four-pad detectors are made on 10 cm polished wafers of float-zone silicon (Wacker, 1997). The wafers are 380μm thick with a rms variation of 5μm (which corresponds to 0.17 charge units at Fe). The thickness variation within wafers is <3.5μm. The silicon is phosphorous-doped with a resistivity of >5000Ω-cm. Three four-pad detectors were made on each wafer. The active areas of the detector pads are 1.945 cm by 1.475 cm so that the whole detector has a seamless active area of 1.945 cm by 5.9 cm. The detectors are PIN diodes. A common blocking contact is created on one side by a phosphorous diffusion while the individual detector pads are created on the other by etching apertures into a silicon dioxide layer. Rectifying contacts are created in these apertures by boron ion implantation. After aluminum contacts are deposited, the whole surface is passivated with silicon dioxide. The finished detectors are tested on wafer with automated probe stations for full depletion and leakage current. After sawing they are tested once more before being mounted on ceramic daughter boards and wire bonded.

2.2 Detector Testing and Selection: Selected daughter boards (DBs) must have a leakage current per detector pad of <100 nA at 100 volts. Also the leakage current should not increase at a rate >3%/volt at 120 volts. The nominal capacitance of each detector pad is 90 pF. All the pads on selected DBs must fully deplete at a bias of <80 volts.

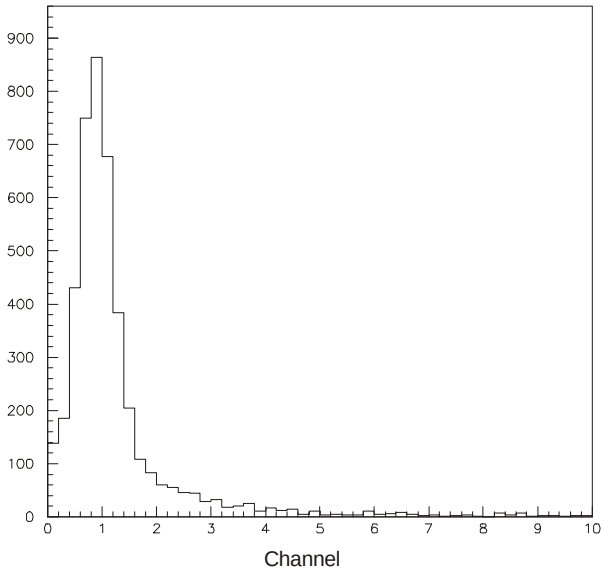

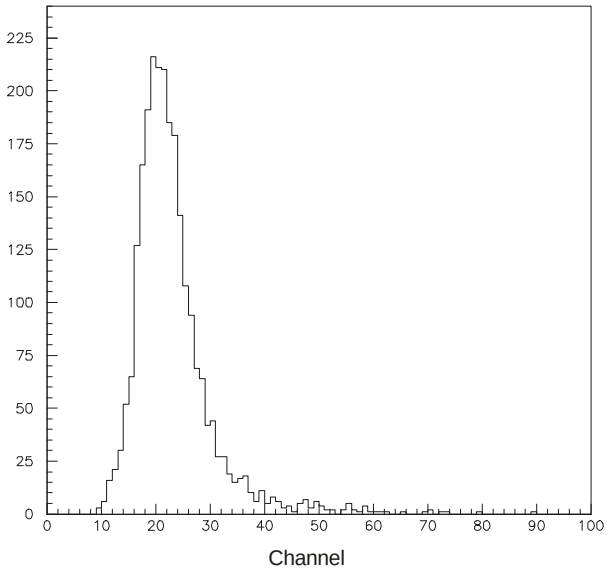

Figure 1: Distribution of detector noise measurements

Figure 2: Typical Electron Beam Spectrum

The noise was measured on DBs that meet the above criteria. Each pad was connected to a preamp, shaper and PHA. Charge pulses were injected at the detector and the pulser peak width was measured. This measurement was repeated with an equivalent capacitor replacing the detector to correct for electronics noise. Figure 1 shows the noise in ~5000 detectors tested. The most probable detector noise is in channel 0.9 (1320 electrons). Detectors with noise <8100 electrons were selected. On many DBs the pads were also checked with a beam of relativistic electrons (2.27≥ E ≥1.5 MeV). Figure 2 shows a typical electron spectrum. The figure shows a Landau distribution with a most probable energy deposition of approximately 111 keV giving a signal of 30,800 electrons. The width of the distribution is primarily due to electronic noise (14 keV) and the natural width of the Landau distribution. Variations in the electron peak location in the detectors tested are consistent with the variation in wafer thicknesses.

3 Detector Electronics:

The 4480 independent detector pads in the matrix must be read out and digitized. ATIC uses a stop-and-read data acquisition system. Triggering is done in two stages. First a fast pre-trigger is generated from the ATIC's plastic scintillators and used to hold the signals. A master trigger identifies events of interest. It must follow the pre-trigger within 2.5 μsec to initiate the readout otherwise the system will reset and wait for the next event.

3.1 Front-end Electronics: There is one front-end channel per detector pad consisting of a charge-sensitive amplifier, a shaping amplifier and a track-and-hold circuit. These reside in 16-channel application-specific integrated circuit (ASIC) chips called CR-1 chips (Adams et al., 1999). The 16 channels are multiplexed to a common output buffer on the chip. Tests of this chip have shown that the rms noise is 4600 electrons.

3.2 Readout Architecture: There are 7 CR-1 chips per motherboard. Following a master trigger, these are multiplexed in turn onto a common data line that leads to a grandmother board (GMB) circuit located outside the matrix. The GMB digitizes the signals and places them in an output register. The GMB also periodically calibrates each channel with accurately known charge pulses. Each GMB has 10 circuits to support

motherboards. It is connected to two ASIC Control Logic Boards (ACLBs) that control data acquisition, calibration, and pedestal measurement. The ACLBs collect the data from the GMB output registers. Each signal is compared to the pedestal measured for that channel. When the signal exceeds a threshold above the pedestal it is buffered into the data system. This sparsification strategy is expected to reduce the data volume by a factor of ~100.

4 Simulated Detector Performance:

The performance of the matrix was simulated using GEANT (Brun et al., 1984). The energy deposition in the silicon detectors was calculated in two parts. The energy loss restricted to the creation of electrons below 10 keV was calculated using the Bethe-Bloch formula. The energy going into higher energy electrons was used to create delta rays that were tracked by GEANT as secondary particles

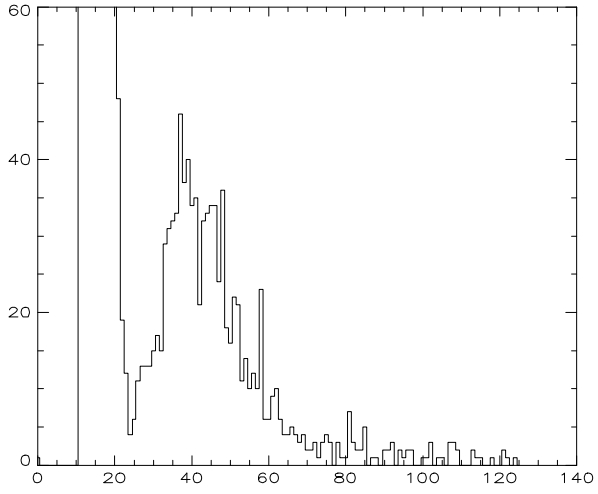

Figure 3: Silicon Matrix spectrum of proton events + noise. The noise spectrum was artificially cut off below channel 1l.

4.1 Sparsification Efficiency: The threshold for keeping a detector signal must be selected to maximize the retention of signals from events without keeping noise. To check this we simulated 100 GeV cosmic ray protons arriving isotropically within the aperture of ATIC. The proton's signal is read along with 4479 noise signals for each event. All the signals include a combined noise of 4700 electrons from the CR-1 chip, the detectors, and the ADC. The proton signals also include the silicon detector thickness variations. Figure 3 shows a simulated spectrum from many such events with the pedestals subtracted. With the threshold set at channel 14, all the protons were detected and 99% of the noise was rejected. Note that event records will contain 45 noise signals, on average, in addition to the proton signal.

4.2 Elemental Resolution: GEANT was used to simulate the energy deposited by protons. The signal from ions of charge Z was simulated by summing the energy deposited by Z^2 protons. Figure 4 shows the simulated charge spectrum for Z = 1 to 28. This spectrum includes a total noise of 4720 electrons and 5 μm detector thickness variations.

4.3 Misidentification: GEANT simulations have shown that the incident particle can be located in the matrix with a rms error of 2 cm above 100 GeV from shower core measurements only. In 2/3 of the cases additional information from the plastic scintillator layers can reduce this to about 1 cm. While the misidentification probabilities have not been estimated for the current detector pad size, estimates were made earlier for 3 cm by 3 cm pixels. Combining these estimates with a 2 cm location error, we estimate that the misidentification probability is 1.4% at 10 TeV. With pixels less than half this size and better locations for 2/3 of the events, we expect the misidentification probability to be smaller at 10 TeV and less than 2% even at 100 TeV.

5 Conclusions:

We have described the first large area silicon matrix developed for cosmic ray research. We have shown the measured detector performance and simulations of the sparsification efficiency, misidentification probability and elemental resolution. The results show that the signals of interest can be separated from noise, and that the design has adequate resolution and background rejection to identify the atomic numbers of the incident cosmic rays from protons to iron.

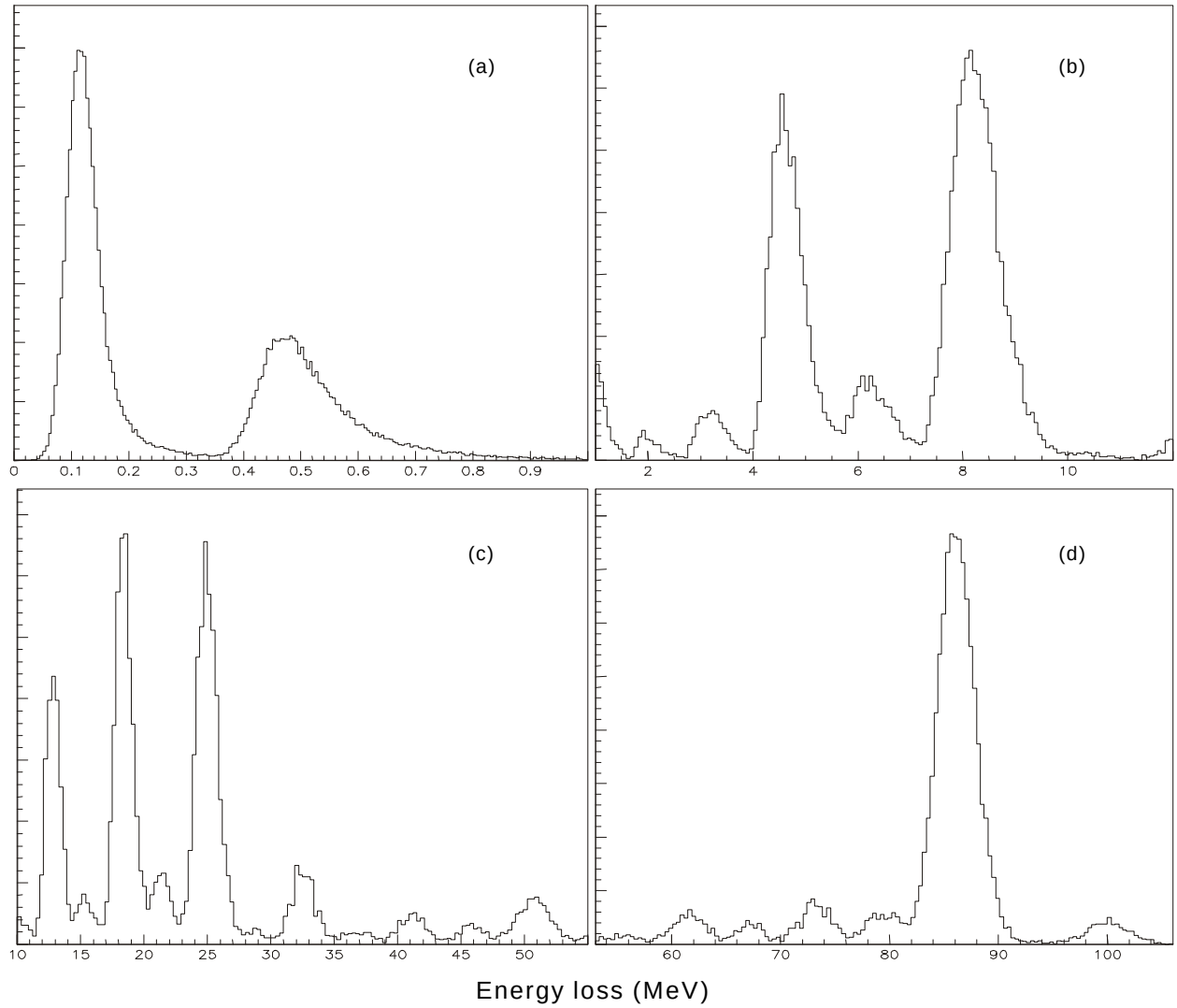

Figure 4: Simulated Charge Resolution of the silicon matrix including all noise sources and detector thickness variations. The charge ranges in the panels are (a) H-He; (b) Li-F; (c) Ne-Ca; and (d): Sc-Ni

References

Adams, Jr., J.H. et al. 1999, paper OG 4.1.18 in this conference

Brun, R. et al. 1984, *User's Guide,* CERN, DD/EE/84-1, Geneva.

Ganel, O. et al. 1999, *in Space Technology and Applications International Forum,* ed. M. El-Genk, AIP Conference Proceedings, **458**, 272-277.

Guzik, T. G. et al. 1999, paper OG 4.1.03 in this conference.

Seo, E. S. et al. 1996, *in Gamma-Ray and Cosmic Ray detectors, Techniques, and Missions,* Ed.by B. D. Ramsey and T. A. Parnell, Proc. SPIE Intl. Symp. on Optical Sci., Eng., and Instr., **2806**, 134-144.

Universal Circuits 1999, 8860 Zachary Lane North, Maple Grove, MN 55369.

Wacker Siltronics 1997, Burghausen, Germany.